

Monitoring the impacts of disruption events on agriculture through irrigation detection with remote sensing

Hasan Siddiqui
Dept. of Mechanical Engineering
 Columbia University
 New York, USA
 hss2152@columbia.edu

Vijay Modi
Dept. of Mechanical Engineering
 Columbia University
 New York, USA
 modi@columbia.edu

Abstract—Adoption of irrigation even on a small scale requires access to suitable soils, sourcing seeds and fertilizers, meeting crop water requirements, energy and infrastructure needed for pumping water and access to markets. Therefore monitoring irrigation over time provides key insight on the effectiveness of policy decisions, infrastructure successes and more importantly, disruptions caused by events such as conflicts, the COVID pandemic etc. All of these have a direct impact on food security. However most of the irrigation maps including coarse global irrigation cropland layers are created for a certain time period and do not reflect changes in the landscape over time. This study presents a simplified alternative to a dry season irrigation detection methodology developed for the Ethiopian highlands that can be implemented using Google Earth Engine’s built in classifiers to create irrigation maps for each year of interest. The original methodology and the proposed simplified approach are compared for a sample region in Oromia to discuss the trade-offs of the simplifications. It is then applied to Southern Tigray across five years from 2019 to 2023 to show how the monitoring technique can be used to visualize the effects of disruptions such as the Tigray War on irrigated agriculture and the recovery efforts after.

Index Terms—irrigation, agriculture, food security, remote sensing, Google Earth Engine

I. INTRODUCTION

The top 10 countries in terms of the total cropland area account for 50 percent of the world’s cropland area. A troubling statistic appears when the 15 year increase in population in these countries which is about 15.5 percent from 2000-2015 is compared with the increase in cropland area during the same time frame which is a mere 2 percent [1]. It is evident that the exhaustion of available agricultural land poses a risk to global food security. This food insecurity is compounded by the effects of climate change which results in unpredictable rainfall pat-

terns which affects the yields of crops due to late or early rains. Irrigation therefore presents itself as a key solution to combating these challenges by supplementing not only the rain-fed agriculture but also increasing the agricultural produce of the land by allowing certain crops to be grown during the dry season.

Numerous studies have shown that irrigation can be linked to not only an increase in income to uplift certain communities from poverty but also an improvement in nutrition. One such study relates an improvement of DHS survey metrics such as height and weight for age with the distance from irrigated crops [2]. The increase in energy consumption from pumping water to meet dry season crop water requirements can be used to provide incentives for grid extension to serve these communities or plan mini-grid and standalone systems with suitable payback periods. This also influences policies that seek to increase the agriculture related economy by planning various scale irrigation schemes and ease the issues related with irrigation namely access to seeds, fertilizers, access to markets and energy requirements.

Several approaches have been utilized in literature to distinguish irrigated agriculture from rain-fed agriculture from comparing different bands of multi-scale remote sensing imagery and indices derived from these bands using two time steps, one in the peak dry season and other in the peak wet season [3] - [5]. Others employ thresholds on the greening indicated from indices to distinguish irrigated crops with little to no soil moisture stress to non-irrigated agriculture crops that experience more moisture stress. These methods are often applicable to certain areas and require either tuning or a

different approach to detect irrigation in other areas. Certain efforts have been made to map irrigation on a global scale at coarser resolutions by combining different methodologies to tackle the challenges to different landscapes [6] - [8]. These are also tuned to reflect the agricultural produce statistics and survey data on existing irrigation schemes [9].

This paper follows a methodology developed for detection of dry season irrigation in the Ethiopian highlands [10]. Dry season irrigation is defined as crops grown in the dry season which is different from irrigation used to supplement crop water requirements in the wet season. The dry season photosynthetic growth is distinguished from evergreen regions that remain green during the dry season. By employing multi-scale imagery, examining Enhanced Vegetation Index (EVI) time series from Sentinel 2 and a transformer model, the methodology is able to detect small-holder irrigated farmlands with an accuracy of 95 percent. The authors showed the effects of the Tigray War which resulted in a significant decrease in irrigated agriculture in Amhara and Tigray by about 40 percent.

However the remarkable model performance of the methodology described comes at a cost of computation resources and requires downloading and processing of imagery for the specified year of interest. The objective of this paper is to simplify the process and utilize the built in Google Earth Engine (GEE) classifiers to predict dry season irrigation and compare the results to the transformer model. The same data used to train the transformer model was utilized for training the classifiers in this paper. This was collected by the authors of this paper and the original methodology with the assistance of other members mentioned in the acknowledgements. GEE has emerged as the tool of choice for land cover monitoring [11]. By simplifying the process, this allows monitoring of irrigated agriculture over time due to implementation of policies, development of irrigation schemes, disruptions due to the COVID pandemic and conflicts etc. and thus can be used to assess the impacts on food security.

The Tigray War which lasted from November of 2020 to November in 2022 resulted in internal displacement of over 2 million people to major cities, de-electrification of electric power grid, destruction of farming equipment depriving the population of income and posing food security challenges. Studies have explored the impact of the conflict incidents on collapse of infrastructure [12] - [13]. A direct impact on vegetation cover decline can be observed through remote sensing due to burning of crops

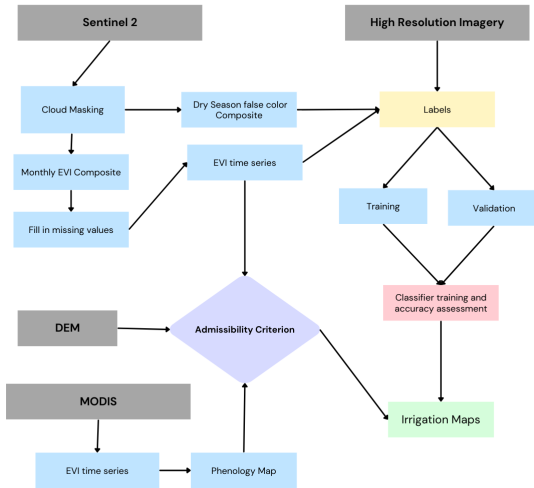


Fig. 1: Flowchart of the methodology

and clearing of woody vegetation. A recent study explored a similar impact of the conflict on cropland in the Ethiopian Highland [14].

II. METHODOLOGY

The simplified methodology proposed for rapid generation of irrigation maps for different years is based on a methodology developed for Ethiopian highlands which forms the baseline to compare the benefits of the simplification steps [10]. A flowchart of the methodology utilized in this study is shown in Fig 1.

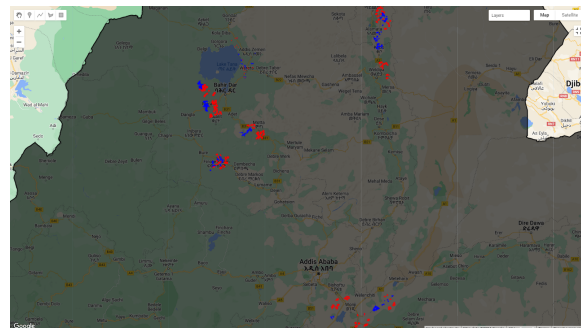


Fig. 2: Irrigated and non-irrigated labels shown with blue and red polygons respectively used for training and testing of classifiers.

A. Label collection for training and validation data

The training data used to train the classifier is generated through the visual inspection of high resolution imagery and Sentinel 2 EVI time series. A phenology map at MODIS 250m scale is used to

characterize the vegetation phenologies. Since dry season irrigation is detected through the study of greening and senescence of croplands in the dry season, it is important to distinguish areas with uni modal rainfall with prolonged dry season from bi modal rainfall areas where the crop growth is dictated by rainfall instead of water requirements met through irrigation techniques. The Sentinel 2 vegetation indices can be replaced by Landsat imagery in Google Earth Engine if needed to access historic datasets that extend before 2017 albeit at the cost of coarser resolution of 30m rather than the Sentinel 2 10m scale which would impact the detection of small-holder farmlands. The baseline methodology utilizes 36 time steps by sampling median composites in the 10-day time period using the two sentinel 2 satellites to provide more accurate changes in the EVI signatures. However in the proposed methodology this is replaced by monthly median composites to aid computational requirements resulting in a total of 12 time steps. The baseline methodology utilizes a Savitsky Golay Filter to smooth and fill in the missing EVI time series due to cloud cover and other issues. This in the proposed methodology is handled through taking the mean of the previous two and the next two EVI values.

For the training step, the polygons with labels are collected through evaluation of different remote sensing products namely Sentinel 2 dry season false color composites made from red SWIR and NIR in the RGB channels, inspection of sub meter resolution imagery from Google and examining of the EVI time series from Sentinel 2. Once the polygons are collected, the time space cube of the EVI are extracted and smoothed. This then in the baseline methodology undergoes a cluster cleaning step in which the time series that do not fit the description of irrigated and non-irrigated time series are discarded. The remaining time series are used to train the classifier. In the proposed methodology, the cluster cleaning step is skipped and all the time series in the polygons are extracted at a scale of 30m and tilescale of 16. This was done for a subset of polygons used in the baseline methodology. The 250 irrigated and 250 non-irrigated polygons were used to generate 657,313 points for training and testing. A 70-30 split was used for training and testing the classifier.

B. Admissibility Criterion

Admissibility criterion are utilized to get rid of the areas where irrigation is unlikely to occur such as highly sloped areas to reduce the computational

resources required for the predictions. A criteria to ensure that the ninetieth percentile of EVI time series are above a certain threshold gets rid of barren areas which show no signs of vegetation throughout the year. If the tenth percentile of EVI time series are below a certain threshold and the ratio of the ninetieth to tenth percentile is greater than 2, this implies that there is no dip in the vegetation index associated with senescence of vegetation or harvesting of the crops. These areas are evergreen regions such as forests, swamps etc that show signs of vegetation throughout the year and thus can be filtered out. These criterion are also implemented in the proposed methodology.

C. Classifiers

The baseline methodology compares the performance of different classifiers and model architectures and shows that the catboost model and the transformer model outperform all the other models. Gradient boosted trees are also an algorithm of choice in remote sensing classification and detection as outlined in the Kaggle AI report 2023. The proposed methodology utilizes the GEE built in random forest classifier to predict irrigated agriculture and compares the model performance to the transformer model as the baseline.

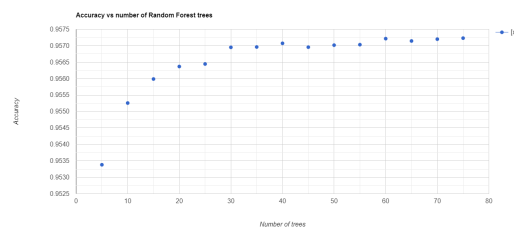


Fig. 3: Hyper-parameter tuning.

III. RESULTS AND DISCUSSION

A random forest classifier with 50 trees was trained on a subset of labeled polygons from Ethiopia and used to predict irrigation for the entire country for 2021. The model achieved an F1 score of 0.888 and an accuracy of 94.66 percent on the irrigated test set and an accuracy of 95.92 percent on the non-irrigated test set. Hyper parameter tuning was performed to select the number of trees. As shown in the Fig. 3, the accuracy does not increase by much after 30 trees used in the random forest classifier. The model was then trained using landsat imagery for 2021 using the same polygons which

resulted in slightly lower F1 score of 0.846, irrigation accuracy of 94.82 percent and non-irrigated accuracy of 94.21 percent over the test set.

A. Comparison of model predictions for Oromia

The transformer model from the baseline methodology was used to predict irrigation for a region in Oromia defined by latitudes 8.20 and 8.72 N and longitudes 3.88 and 3.90 E for 2021. The results were then used to compare another batch of irrigation predictions made using the proposed simplified methodology in Earth Engine. Visual inspection of the results reveal that the random forest classifier over-predicts irrigation in certain areas. The GEE model predicts 302 sq km of the 6206 sq km as irrigated whereas the transformer model predicts only 160 sq km as irrigated. An examination of EVI time series in areas that were wrongly predicted as irrigated reveals that it is due to false spikes in the EVI time series due to cloud cover issues missed through masking. In the baseline methodology, these are smoothed using the Savitsky Golay filter. This degradation in performance is therefore attributed to using fewer time steps and using the mean of adjacent month values to fill in missing gaps instead of a smoothing function.

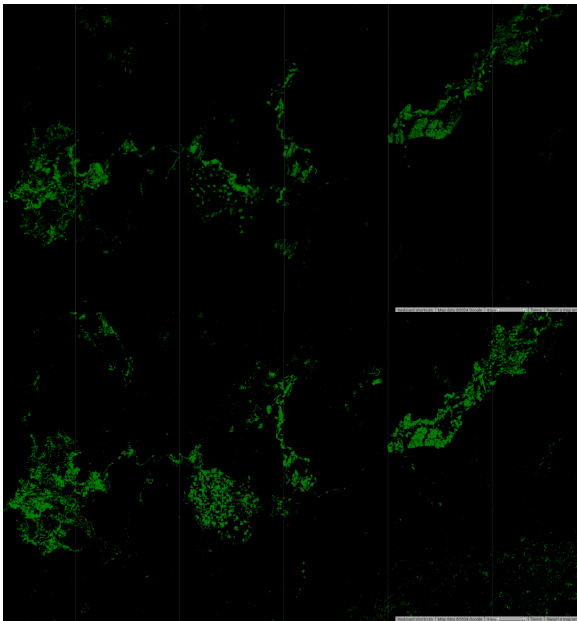


Fig. 4: Irrigation Prediction comparisons for Oromia 2021 for transformer model (top) and random forest model (bottom). Irrigation predictions are shown by green pixels.

B. Irrigation detection in Southern Tigray

The random forest classifier model was then used to predict irrigation in Southern Tigray over 5 years from 2019 to 2023 to assess the impacts of the Tigray War, pandemic and recovery efforts after the conflict. These are shown in Fig.6 with zoomed in views of Mekele City in 2019 and 2023.

In 2019, the total irrigated area was 714 sqkm which increased to 740 sq km the next year despite the COVID pandemic. However a significant reduction in irrigated areas is observed by roughly 63 percent to 276 sq km in the year 2021 due to the Tigray War. No significant change is observed in 2022 in which the total irrigated area is 265 sqkm. In the year 2023 following the end of the war, the irrigated area has increases by roughly 10 percent to 820 sq km from 2020.

The massive increase in irrigated area in 2023 can be explained by two factors. Towards the northern part of the region in Mekele City, an influx of displaced people triggered a boom in urban agriculture which is evident by comparing the 2019 and 2023 irrigation maps [15]. Another huge change responsible to most of this irrigation increase is visible in the south. This area along with eastern Amhara, eastern Oromiya and north-eastern SNNP regions experienced abundant seasonal rainfall from February to May with up to twice the long-term average. This hugely increased the secondary "Belg" season crops. This is reported by the Agricultural Stress Index for cropland map for Ethiopia during this time frame by the Food Agriculture Organization of the United Nations [16]. While this agriculture production increase is not dry season irrigation, the model has not been trained to distinguish for such anomalies and therefore exposes the limitations of the methodology.

IV. CONCLUSION AND RECOMMENDATIONS

The simplified model was applied as an alternative to the transformer model developed for small-holder irrigation detection in the Ethiopian highlands [10]. Results showed a comparative performance of the GEE classifier model to the superior neural network over the testing dataset. However predictions revealed that the random forest model was over-predicting the dry season irrigation in certain regions. Despite this, the model allows rapid detection of irrigated croplands across different years. Even though the classifier is trained for a specific year in this case 2021, it can be applied to other years. Using Landsat, trends preceding 2017 where the Sentinel 2 satellites do not have coverage,

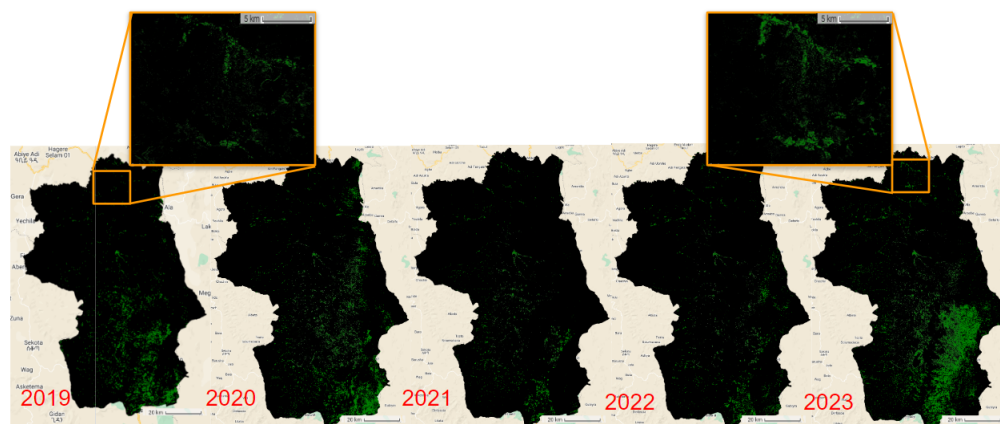


Fig. 5: Irrigation predictions in green for Southern Tigray for 5 years from 2019 to 2023 respectively. Mekele City area zoomed in for 2019 and 2023

can be studied. From the predictions shown across Southern Tigray across several years, the effects of the conflict can be observed as a decrease in the irrigated agriculture from 2020 to 2021 due to equipment that has been destroyed and farms that have been burnt. Then in 2023, an increase in irrigated agriculture is observed mostly due to unusually high rainfall from Feb-May in the south.

The model was then applied to the entire country and a section of the irrigation predictions spanning Amhara, Tigray and parts of Oromia is shown in the Fig. 6. The model predicts a lot more irrigated area in the southern part of the country. This is not due to lack of labels in this area but due to the nature of vegetation phenologies that dominate this region. The indigenous vegetation in this area shows a double greening and senescence cycle following the bimodal rainfall this region receives. This model interprets this as irrigated agriculture due to the similar nature of dual cropping cycles. This calls for a separate methodology to tackle the irrigation detection in this region but the dry season irrigation detection can be masked out by using a threshold on the dual cropping cycles in phenology map.

CODE AVAILABILITY

The Google Earth Engine script used for the results in this paper is available at Github at github.com/hssiddiqui/IEEE-GHTC-24-Irrigation-Monitoring

ACKNOWLEDGMENT

The authors would like to acknowledge Terence Conlon for providing the the code and labels to replicate the transformer results in Oromia and also Jack Bott, Yinbo Hu, and Yuezi Wu for assistance

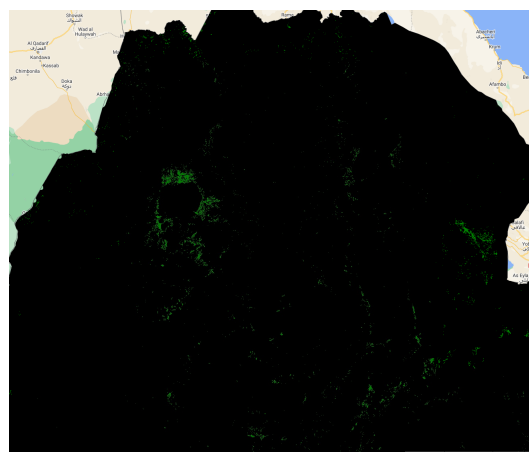


Fig. 6: Irrigation predictions shown in green for Amhara, Tigray and parts of Oromia in Ethiopia for 2021.

in collecting labels that were used for training the classifier in Google Earth Engine.

REFERENCES

- [1] P. S. Thenkabail et al., "Global cropland-extent product at 30-m resolution (GCEP30) derived from Landsat satellite time-series data for the year 2015 using multiple machine-learning algorithms on Google Earth Engine cloud," Reston, VA, Report 1868, 2021. doi: 10.3133/pp1868.
- [2] A. BenYishay et al., "Irrigation strengthens climate resilience: Long-term evidence from Mali using satellites and surveys," *PNAS Nexus*, vol. 3, no. 2, p. pgae022, Feb. 2024, doi: 10.1093/pnasnexus/pgae022.
- [3] J. Magidi, L. Nhamo, S. Mpandeli, and T. Mabhaudhi, "Application of the Random Forest Classifier to Map Irrigated Areas Using Google Earth Engine," *Remote Sensing*, vol. 13, no. 5, p. 876, Feb. 2021, doi: 10.3390/rs13050876.
- [4] M. Vogels, S. De Jong, G. Sterk, H. Douma, and E. Addink, "Spatio-Temporal Patterns of Smallholder Irrigated Agriculture in the Horn of Africa Using GEOBIA and Sentinel-

- 2 Imagery,” *Remote Sensing*, vol. 11, no. 2, p. 143, Jan. 2019, doi: 10.3390/rs11020143.
- [5] H. A. Zurqani, J. S. Allen, C. J. Post, C. A. Pellett, and T. C. Walker, “Mapping and quantifying agricultural irrigation in heterogeneous landscapes using Google Earth Engine,” *Remote Sensing Applications: Society and Environment*, vol. 23, p. 100590, Aug. 2021, doi: 10.1016/j.rsase.2021.100590.
- [6] F. T. Portmann, S. Siebert, and P. Döll, “MIRCA2000—Global monthly irrigated and rainfed crop areas around the year 2000: A new high-resolution data set for agricultural and hydrological modeling,” *Global Biogeochemical Cycles*, vol. 24, no. 1, p. 2008GB003435, Mar. 2010, doi: 10.1029/2008GB003435.
- [7] P. S. Thenkabail et al., “Global irrigated area map (GIAM), derived from remote sensing, for the end of the last millennium,” *International Journal of Remote Sensing*, vol. 30, no. 14, pp. 3679–3733, Jul. 2009, doi: 10.1080/01431160802698919.
- [8] S. Siebert, V. Henrich, K. Frenken, and J. Burke, Update of the digital global map of irrigation areas to version 5. 2013. doi: 10.13140/2.1.2660.6728.
- [9] “AQUSTAT.” [Online]. Available: <https://data.apps.fao.org/aquamaps>
- [10] T. Conlon, C. Small, and V. Modi, “A Multiscale Spatiotemporal Approach for Smallholder Irrigation Detection,” *Front. Remote Sens.*, vol. 3, p. 871942, Apr. 2022, doi: 10.3389/frsen.2022.871942.
- [11] G. Azzari and D. B. Lobell, “Landsat-based classification in the cloud: An opportunity for a paradigm shift in land cover monitoring,” *Remote Sensing of Environment*, vol. 202, pp. 64–74, Dec. 2017, doi: 10.1016/j.rse.2017.05.025.
- [12] F. B. Tekulu, “The effect of war on basic infrastructures of Eastern Tigray, Ethiopia,” *GeoJournal*, vol. 89, no. 1, p. 39, Feb. 2024, doi: 10.1007/s10708-024-11041-6.
- [13] E. Negash et al., “Remote sensing reveals how armed conflict regressed woody vegetation cover and ecosystem restoration efforts in Tigray (Ethiopia),” *Science of Remote Sensing*, vol. 8, p. 100108, Dec. 2023, doi: 10.1016/j.srs.2023.100108.
- [14] L. Weldegebriel, E. Negash, J. Nyssen, and D. B. Lobell, “Eyes in the sky on Tigray - Monitoring the impact of armed conflict on cultivated highland using satellite imagery in Ethiopia.” *Science of Remote Sensing*, p. 100133, May 2024, doi: 10.1016/j.srs.2024.100133.
- [15] B. O’Donovan-Iland, “How war and crises in Tigray triggered an urban agriculture boom,” *Institute of Development Studies*, Aug. 02, 2023. <https://www.ids.ac.uk/opinions/how-war-and-crises-in-tigray-triggered-an-urban-agriculture-boom/> (accessed May 3, 2024)
- [16] “FAO GIEWS Country Brief on Ethiopia -,” www.fao.org/giews/countrybrief/country.jsp?code=ETH